PHYSICAL REVIEW B, VOLUME 63, 245307

# Strain relaxation in (0001) AlN/GaN heterostructures

Alain Bourret,[1] Christoph Adelmann,[1] Bruno Daudin,[1,*] Jean-Luc Rouvière,[1] Guy Feuillet,[1] and Guido Mula[1,2]
[1]Commissariat à l'Energie Atomique/Grenoble, Département de Recherche Fondamentale sur la Matière Condensée, Service des Matériaux et Microstructures Grenoble, 17 rue des Martyrs, 38054 Grenoble Cedex 9, France
[2]Instituto Nazionale di Fisica della Materia and Dipartimento di Fisica, Università di Cagliari, Cittadella Universitaria, Strada Provinciale Monserrato-Sestu km 0.700, 09042 Monserrato (CA), Italy

(Received 23 October 2000; published 4 June 2001)

The strain-relaxation phenomena during the early stages of plasma-assisted molecular-beam epitaxy growth of lattice-mismatched wurtzite (0001) AlN/GaN heterostructures have been studied by real-time recording of the *in situ* reflection high-energy electron diffraction (RHEED), *ex situ* transmission electron microscopy (TEM), and atomic-force microscopy. A pseudo-two-dimensional layer-by-layer growth is observed at substrate temperatures of 640–660 °C, as evidenced by RHEED and TEM. However, the variation of the in-plane lattice parameter during growth and after growth has been found to be complex. Three steps have been seen during the deposition of lattice-mismatched AlN and GaN layers: they were interpreted as the succession of the formation of flat platelets, 3–6 monolayers high (0.8–1.5 nm) and 10–20 nm in diameter, their partial coalescence, and gradual dislocation introduction. Platelet formation leads to elastic relaxation as high as 1.8%, i.e., a considerable part of the AlN/GaN lattice mismatch of 2.4%, and can be reversible. Platelets are always observed during the initial stages of growth and are almost insensitive to the metal/N ratio. In contrast, platelet coalescence and dislocation introduction are very dependent on the metal/N ratio: no coalescence occurs and the dislocation introduction rate is higher under N-rich conditions. In all cases, the misfit dislocation density, as measured by the irreversible relaxation, is initially of the order of $7\times10^{11}\,\mathrm{cm}^{-2}$ and decreases exponentially with the layer thickness. These results are interpreted in the framework of a model that emphasizes the important role of the flat platelets for dislocation nucleation.

DOI: 10.1103/PhysRevB.63.245307 PACS number(s): 68.55.−a, 61.72.Lk, 81.40.Lm

## I. INTRODUCTION

The epitaxial growth of complex semiconductor heterostructures, such as quantum wells, quantum dots, or superlattices, has become of paramount importance in the context of producing high-performance electronic and optoelectronic devices. Especially III-V nitride compounds are a material system that has been the subject of intense work in the recent past due to the possibility to achieve blue or ultraviolet light-emitting and laser diodes,[1,2] blue resonant-cavity light-emitting diodes[3] and surface-emitting lasers,[4,5] and solar-blind ultraviolet photodetectors,[6–8] as well as high-power high-frequency field-effect transistors.[9–11]

However, in GaN/AlN heterostructures the lattice mismatch is of the order of 2.4% and large strain builds up.[12,13] This raises the question of strain relaxation even for thin epitaxial GaN or AlN layers. Moreover, it has been established that the optical properties of III-V nitride heterostructures, e.g., GaN/$\mathrm{Al}_x\mathrm{Ga}_{1-x}$N quantum wells[14–16] or GaN/AlN quantum dots,[17,18] are significantly modified by strain-induced piezoelectric polarization. Thus, the investigation of strain and strain relaxation is important not only for understanding the structural but also the optical properties of III-V nitride heterostructures.

Whereas nucleation and strain evolution have been intensively studied for the growth of GaN and AlN on sapphire substrates,[19–29] this is less the case for nitride heterostructures.[30–35] Up to now, most of the published contributions are on measurement of the strain and strain relaxation with only few elaborations upon the actual mechanism involved for relaxation.[22,23] It has been shown that growth by plasma-assisted molecular-beam epitaxy (PAMBE) of GaN on AlN follows a Stranski-Krastanow mode at high temperatures, i.e., the strain is elastically relaxed on the free surface of islands, while it is layer-by-layer growth at lower temperatures.[36]

The purpose of this article is to study the relaxation processes active in wurtzite (0001) AlN/GaN multilayers grown by PAMBE at low temperature, for which the growth is layer by layer. It will be shown that the usual concept of a ''critical thickness'' for introducing dislocations as originated by Matthews and Blakeslee[37] and People and Bean[38] is not operative. It will be further demonstrated that the initial relaxation occurs via a three-step mechanism consisting of the following: (1) the dynamic formation of planar platelets, not necessarily observable *ex situ*; (2) their partial coalescence, and, finally; (3) the formation of dislocations, most likely at the edges of the platelets. This will explain the various values of the ''critical thickness'' reported in the literature.

## II. EXPERIMENTAL DETAILS

The samples were grown by PAMBE in a MECA 2000 chamber, at growth rates of about 300 nm/h, i.e., 0.3 monolayers/s. Standard Knudsen cells were used for gallium and aluminum evaporation and active nitrogen was generated by a radio frequency (rf) plasma cell from EPI Company. The pseudosubstrates were (0001) (Ga-polarity) GaN layers grown by metal-organic vapor phase epitaxy (MOVPE) on sapphire, about 1.5 $\mu$m thick. These pseudosubstrates were overgrown *in situ* by GaN buffer layers, at least 50 nm thick, to prevent the possible influence of a substrate surface oxide

 ©2001 The American Physical Society

or contamination layer. For some samples described below, a relaxed AlN layer was subsequently deposited, typically 300 nm thick, and used as a pseudosubstrate to study the growth of GaN on AlN. The degree of relaxation of the AlN pseudosubstrate is never complete and care should generally be taken to deduce the initial lattice parameter experienced by the first deposited layer.

Two types of structures were studied: (a) A single layer of GaN and AlN, on relaxed AlN and GaN substrates, respectively. Typically these layers were, after complete growth, at least 20 nm thick. (b) AlN/GaN superlattices with thicknesses varying from nominally 3.2 nm/3.2 nm to 5.0 nm/5.0 nm, both on AlN and GaN substrates.

All layers were grown in the substrate temperature range most suitable for maintaining two-dimensional (2D) Frank–van der Merwe growth for both GaN and AlN, i.e., $T_S = 640-660\,°\mathrm{C}$. For higher substrate temperatures, $T_S \geqslant 680\,°\mathrm{C}$, Stranski-Krastanow growth takes over for GaN on AlN, whereas the growth of AlN on GaN remains 2D.[36]

An important parameter of GaN and AlN growth by PAMBE is the metal/nitrogen flux ratio $\Phi_{\mathrm{III}}/\Phi_{\mathrm{N}}$ (III=Al, Ga). As it is difficult to estimate the active nitrogen flux $\Phi_{\mathrm{N}}$, we usually work at fixed plasma-cell conditions [0.5 standard cubic centimeters per minute (sccm) $N_2$, 300 W rf power for all experiments described below] and adjust appropriately the Ga flux $\Phi_{\mathrm{Ga}}$ or the Al flux $\Phi_{\mathrm{Al}}$ to obtain metal- or N-rich growth.

When the growth of GaN is carried out on a N-rich surface, it has been calculated that the diffusion barrier for Ga atoms is as high as 1.8 eV, whereas it is only 0.4 eV when the growth is carried out on a Ga-saturated surface.[39] In the N-rich case, the large diffusion barrier leads to an undesired kinetically induced roughening of the GaN surface during growth.[40,41] The phenomenology is essentially identical for AlN. Therefore, as concerns PAMBE, GaN and AlN are generally deposited under slightly metal-rich conditions. At the growth temperatures used in the present study, this leads to metal accumulation at the surface. Therefore, growth interruptions under nitrogen flux are usually performed to consume the excess metal. In particular, this is done after every layer of the superlattices considered in this article. The effect of growth interruptions under active nitrogen flux and of growth stoichiometry on the corrugation and relaxation of the surface will be discussed below.

The growth process and mode is monitored by a digitized reflection high-energy electron diffraction (RHEED) pattern. The relative variation of the in-plane lattice parameter of the top layers $\Delta a/a$ is measured as a function of the deposition time on the RHEED pattern by evaluating the distance of the (10) and $(\bar{1}0)$ RHEED streaks in the $[11\bar{2}0]$ azimuth. For this purpose, the position of the streaks is determined by Gaussian fits. The accuracy of the relative lattice parameter variation is typically better than $\pm 0.05\%$.

Transmission electron microscopy at 400 keV in the high-resolution mode (HRTEM) was performed on cross sections: the interfaces as well as the thickness of the deposited layers could be studied at a 0.25-nm scale. *Ex situ* atomic-force microscopy (AFM), operated in the tapping mode, gave the surface corrugation of the layers after interruption of deposition, rapid sample cooling, and transfer into air.

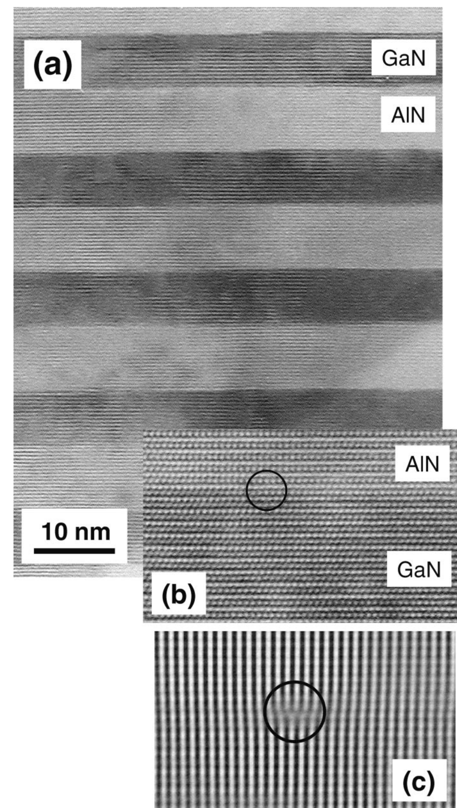


FIG. 1. Transmission electron micrograph of a 7.0 nm/9.3 nm GaN/AlN superlattice. (a) general view, (b) atomic imaging showing perfect coherency at the interface except for one dislocation well visible on filtered image (c). Zone axis $\langle 2\bar{1}\bar{1}0\rangle$.

A typical image of a HRTEM cross section of a 7.0 nm/9.3 nm GaN/AlN superlattice, grown under both Ga- and Al-rich conditions, is displayed in Fig. 1(a). It shows that 2D growth seems well under control and that interfaces are relatively sharp. Quantitative measurements of the interfacial quality have shown that the AlN on GaN interface is larger by one monolayer (ML) than the corresponding GaN on AlN interface.[42] It will be shown below that the dynamic situation is far more complicated than these direct *ex situ* observations would suggest.

## III. GROWTH OF AlN ON GaN SUBSTRATE

### A. Single layer

The evolution of the in-plane lattice parameter of a single AlN layer grown at $T_S = 660\,°\mathrm{C}$ is shown in Fig. 2 as a function of deposition time. The growth conditions have been varied from AlN-rich [Fig. 2(a)] to N-rich [Fig. 2(c)]. Generally, three variation regimes can be distinguished: (A) a sudden drop during the first 2 or 3 ML (0.5–0.75 nm) deposited, (B) for some conditions, a plateau or an increase during the next 5 nm, and (C) a slow and constant decrease towards the AlN value.

Typically, the amplitude of the drop in stage (A) is 0.7–0.9%; in some cases a larger value up to 1.8% is found. However, as a whole, stage (A) seems to be rather independent of the Al/N ratio.

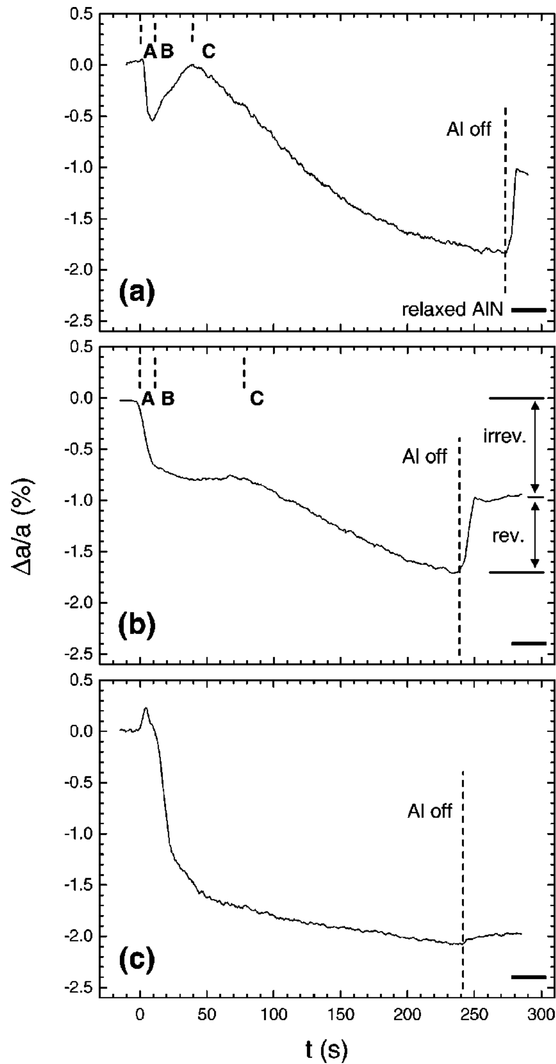


FIG. 2. Relative variation of the in-plane lattice parameter $\Delta a/a$ as a function of deposition time $t$ during the growth of a single layer of AlN on GaN substrate. (a) Al-rich, (b) stoichiometric, and (c) N-rich conditions. After AlN deposition, the Al flux is stopped, and the sample is hold under N flux alone, as indicated. The three steps (A), (B), and (C) are well distinguished in (a) and (b). $T_S = 640\,°C$; the growth rate is 0.3 ML/s for (a) and (b) and 0.2 ML/s for (c), except after the metal flux is interrupted.

Stage (B) is extremely dependent on the exact Al/N stoichiometry: for Al-rich growth [$\Phi_{Al}/\Phi_N = 1.1$, Fig. 2(a)], after the drop, an increase in $a$ almost up to the initial value is observed, followed by the decrease of stage (C). When stoichiometry ($\Phi_{Al}/\Phi_N = 1.0 \pm 0.03$) is approached [Fig. 2(b)] the increase is substituted by a constant plateau. For these two growth conditions [Figs. 2(a) and 2(b)], the ''critical thicknesses'' before stage (C) occurs can be rather well distinguished and are evaluated to be 3 and 6 nm, respectively.

Note that under Al-rich conditions the RHEED pattern is only slightly affected during these changes, i.e., it remains streaky, signaling that apparent 2D growth is preserved. In fact, both persistent specular RHEED intensity as well as in-plane lattice parameter oscillations are observed in the plateau region (Fig. 3). This unambiguously indicates that the growth is layer-by-layer under these conditions.

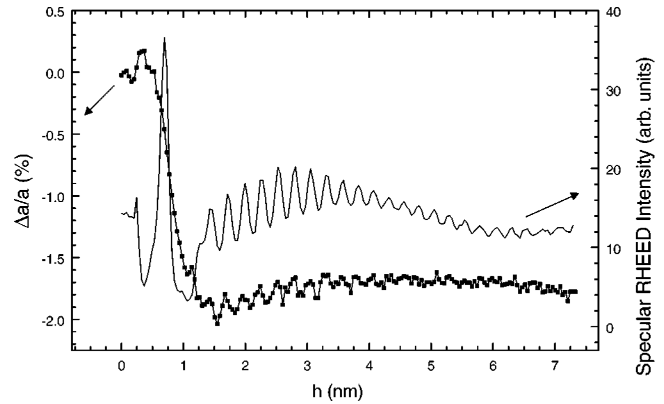


FIG. 3. Relative variation of the in-plane lattice parameter $\Delta a/a$ and specular RHEED intensity as a function of layer thickness $h$ during the deposition of a single AlN layer on a GaN substrate at $T_S = 640\,°C$. Oscillations, characteristic of a layer-by-layer growth, are visible on both signals.

As the $\Phi_{Al}/\Phi_N$ ratio is slightly further reduced to 0.6 [N-rich growth, Fig. 2(c)], stage (B) disappears and $a$ evolves rapidly towards the relaxed AlN value at $-2.4\%$. Stages (B) and (C) are not well-defined. Therefore, no critical thickness can be assessed. Here, the RHEED pattern changes gradually from streaky to spotty during growth, since kinetic surface roughening due to high diffusion barriers for Al adatoms occurs, as mentioned above. The thickness scale for kinetic roughening is of the order of several nanometers and is thus much longer than that for platelet formation, which is of the order of 2–3 ML (0.5–0.75 nm).

When the Al flux is interrupted and the active N flux is maintained, the in-plane lattice parameter recovers part of its initial value, showing that the relaxation process contains two contributions: one irreversible and one reversible. The reversible part is very dependent on the Al/N ratio: it is maximum for Al-rich conditions, lower around stoichiometry, and can be completely suppressed in N-rich conditions.

### B. Superlattice

If one now considers a superlattice with alternate and equally 5-nm-thick GaN and AlN layers grown on the same GaN substrate (Fig. 4 for metal-rich AlN and GaN growth; Fig. 5 for Ga-rich GaN and N-rich AlN growth). Steps (A) and (B) are well visible during growth, while step (C) is not visible as the AlN layer thickness is insufficient. After the interruption of the Al flux (nitrogen flux only) and as observed before, the in-plane lattice parameter recovers most of its original value when AlN growth has previously been carried out under Al-rich conditions (Fig. 4). Under N-rich conditions the recovery is not observed (Fig. 5). This process is pseudoperiodic and reappears at each period of the superlattice: the only change is a gradual and irreversible decrease of the in-plane lattice parameter to the fully relaxed value of a superlattice with equal AlN and GaN layer thicknesses, i.e., 1.3%. No clear correlation of the maximum in-plane lattice parameter change with the misfit experienced by AlN (varying from one period to the next) has been established.

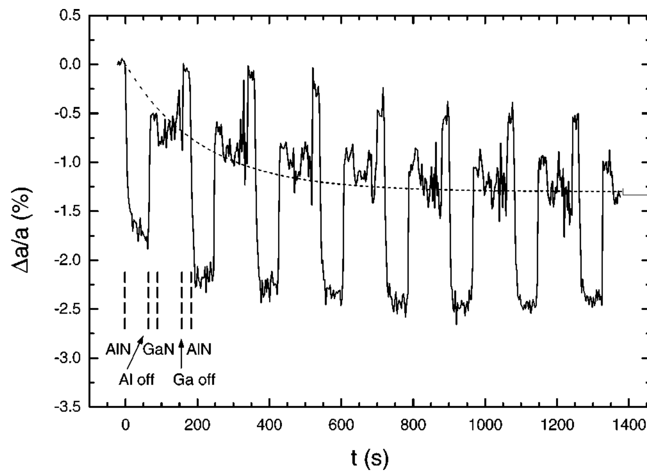


FIG. 4. Relative variation of the in-plane lattice parameter as a function of deposition time $t$ during the growth of a 5.0 nm/5.0 nm AlN/GaN superlattice on a GaN substrate. Al- and Ga-rich conditions, $T_S = 640\,^{\circ}\mathrm{C}$. Note that an interruption of metal deposition during 20 s is carried out after each layer deposition. The growth rate is 0.3 ML/s, except after the metal flux is interrupted. The gradual irreversible relaxation due to dislocation introduction is evidenced with a dotted line.

### C. Reversible and irreversible relaxations

From these observations, it is clear that part of the observed change in the in-plane lattice parameter is reversible and is due to an ''apparent'' relaxation process. This phenomenon was previously observed in the Ge/Si system.[43] The proposed explanation is that the relaxation is due to discontinuities in the 2D layer. Platelets, a few monolayers high, are the possible origin of elastic relaxation at their border. In fact, lateral inward (outward) elastic relaxation of finite platelets strained in tension (compression) is a well-known phenomenon.[44–46]

The observation of a pseudo-2D growth is understood by the fact that these platelets are flat and form a dense network with a coverage close to 1. This is confirmed by the observations of oscillations of the specular RHEED intensity as

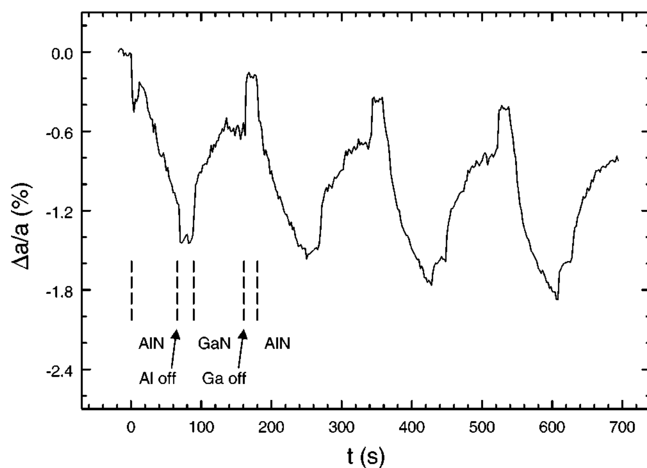


FIG. 5. Same as Fig. 4, but AlN growth is carried out under N-rich conditions.

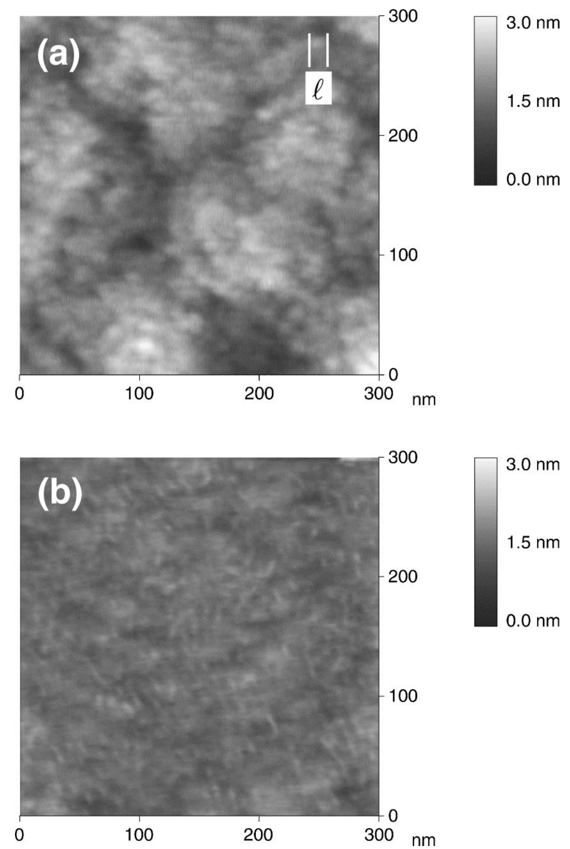


FIG. 6. AFM image of the top surface after growth of a 4-nm-thick AlN layer on GaN substrate (a) N-rich conditions, (b) Al-rich conditions, $T_S = 640\,^{\circ}\mathrm{C}$. 2–3-ML high AlN islands of typical diameter $l = 20$ nm are observed for N-rich growth while a flat surface is observed under Al-rich conditions presenting a disordered array of mono- and bimolecular steps.

well as of the in-plane lattice parameter (Fig. 3): on the planar top surface of each platelet, the growth mode continues to be layer-by-layer, similar to what has been observed for III-V arsenides[47] and II-VI tellurides.[48]

The *ex situ* observation of the dynamic corrugations occurring during growth is difficult: they disappear during the stopping of the Al deposition in Al-rich conditions. The only option is to grow under N-rich conditions, stop the Al deposition, and image the surface on which elastic apparent relaxation is still present. On AFM micrographs, corrugations, about 2–3 ML high, at a scale of $l = 20$ nm are visible [Fig. 6(a)]. However, they are completely absent for Al-rich conditions [Fig. 6(b)]. In the latter case, a disordered array of steps of mono- and bimolecular height is observed.

The same phenomenology is observed on HRTEM on a 4-nm-thick AlN layer grown at $T_S = 720\,^{\circ}\mathrm{C}$: platelets in a planar film are well visible (Fig. 7). The height of the discontinuities is difficult to determine but is at minimum 2–3 ML's. Although not directly comparable to the AFM micrograph due to the higher growth temperature, the HRTEM image well illustrates the occurrence of platelets.

At this point the qualitative interpretation of the three steps in the apparent relaxation process during growth are the following: (A) dynamic platelet formation right from the be-

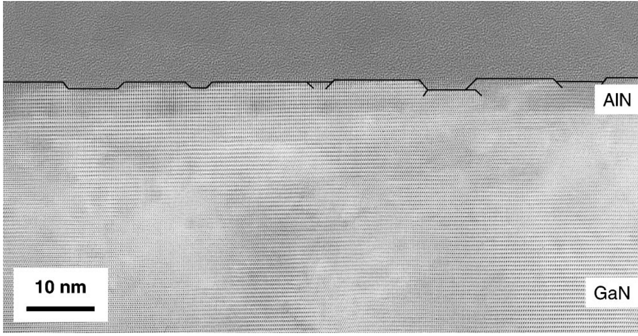


FIG. 7. HRTEM cross section of a 4-nm-thin AlN layer, deposited in nearly stoichiometric conditions ($\Phi_{Al}/\Phi_N = 1.0 \pm 0.03$) at $T_S = 720\,°C$. Although grown at a temperature higher than samples in Figs. 1–6, flat platelets are still visible. The shape is more pronounced and more visible by HRTEM at this temperature. The approximate shape of each platelet is outlined for sake of clarity.

ginning, (B) a dynamic stationary regime with floating islands on top of the growing layer near stoichiometry or gradual island coalescence for Al-rich growth, and (C) irreversible introduction of dislocations. It is interesting that stage (A) appears rather independent of the Al/N ratio, in contrast to stage (B). This may be explained on one hand by the fact that in all experiments, AlN growth is started on a N-rich $2\times 2$-reconstructed GaN surface. On the other hand, it is reasonable to assume that the change in metal-adatom diffusion between N-rich and metal-rich surfaces[39] takes place for a finite metal-surface coverage. Then, for metal-rich growth conditions, the surface kinetics become ''time-dependent'': in the beginning, diffusion is low since the surface is still N-rich; during the growth, metal is accumulated on the surface, and after a finite time depending on the metal excess, a critical surface coverage is attained that modifies surface kinetics and increases metal-adatom diffusion. Hence, it becomes understandable that stage (A) is independent of the exact Al/N ratio, since it occurs in the very beginning of the growth when the surface is always (at least transiently) N-rich. If $\Phi_{Al} > \Phi_N$, the surface will become gradually Al-rich and the adatom diffusion will be altered at a finite critical metal surface coverage. As a consequence, the relaxation during stage (B) becomes dependent on the growth stoichiometry, as discussed above.

After stopping the Al flux, the top surface reappears coherent to the substrate (apart from the irreversible part due to dislocation introduction) so that most of the gaps between platelets are filled. The presence of a continuous surplus Al film on top of the growing layer under Al-rich conditions could explain both the gradual smoothing and filling process under nitrogen flux: the consumption of the Al top layer helps to smooth the film. This process explains the reversible relaxation process.

Quantitative measurement of the irreversible relaxation occurring during step (C) is summarized in Table I. It has been evaluated through the characteristic thickness $\Lambda$ at which a fraction of $1-1/e$ of the irreversible relaxation has occurred. This evaluation will be further elaborated below. It is worth noticing that irreversible relaxation is fastest in N-rich conditions. Some of the dislocations participating to the step (C) were observed by HRTEM at the AlN on the GaN interface [edge-type in-plane dislocations as illustrated in Figs. 1(b) and 1(c)].[42]

TABLE I. Characteristic length $\Lambda$ and total amplitude $\epsilon_0$ of the irreversible relaxation for AlN and GaN layers under different growth conditions.

| Sample | $\Phi_{III}/\Phi_N$ | $\Lambda$ (nm) | $\epsilon_0$ (%) |
|---|---|---|---|
| AlN on GaN substrate | 1.1 | 9.0 | 2.3 |
| | 1.0 | 15 | 1.7 |
| | 0.8 | 5.5 | |
| | 0.6 | 3.5 | |
| GaN on AlN substrate | 1.1 | 12 | $\geqslant 1.3$ |

## IV. GROWTH OF GaN ON AN AlN SUBSTRATE

### A. Single layer

The variation of the in-plane lattice parameter $a$ during deposition of a thick GaN layer on AlN is shown in Fig. 8. The growth has been carried out at $T_S = 640\,°C$ under slight Ga-excess conditions. As for the case of AlN on GaN, one can distinguish three stages: (A) a sudden increase of 1.1% to 1.3% during the first 2 or 3 ML (0.5–0.75 nm) deposited, (B) a rapid decrease during the next 0.5 to 1.4 nm almost to the initial level, and (C) a subsequent slow increase.

While stage (A) is almost independent of the Ga/N ratio, stage (B) has been found to be very sensitive to growth stoichiometry. Figure 9 displays the variation of $a$ at early deposition time for different Ga/N ratios: (a) Ga-rich, (b) approximately stoichiometric, and (c) N-rich growth. For Ga-rich conditions, a rapid increase of $a$ (stage A), followed by a decrease [stage (B)] is observed. Note that the initial value of $a$ is then recovered, corresponding to a completely strained GaN layer, coherent to the AlN pseudosubstrate. For N-rich conditions, stage (B) is completely absent, i.e., we observe a

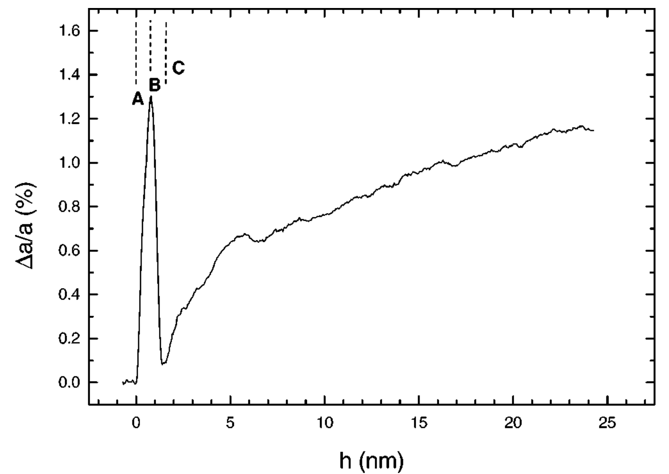


FIG. 8. Relative variation of the in-plane lattice parameter as a function of layer thickness $h$ during the growth of a single GaN epilayer on AlN. Ga-rich conditions, $T_S = 640\,°C$. Note the large relaxation occurring in the first 3–4 ML [step (A)], followed by rapid smoothing [step (B)], and dislocation introduction [step (C)].

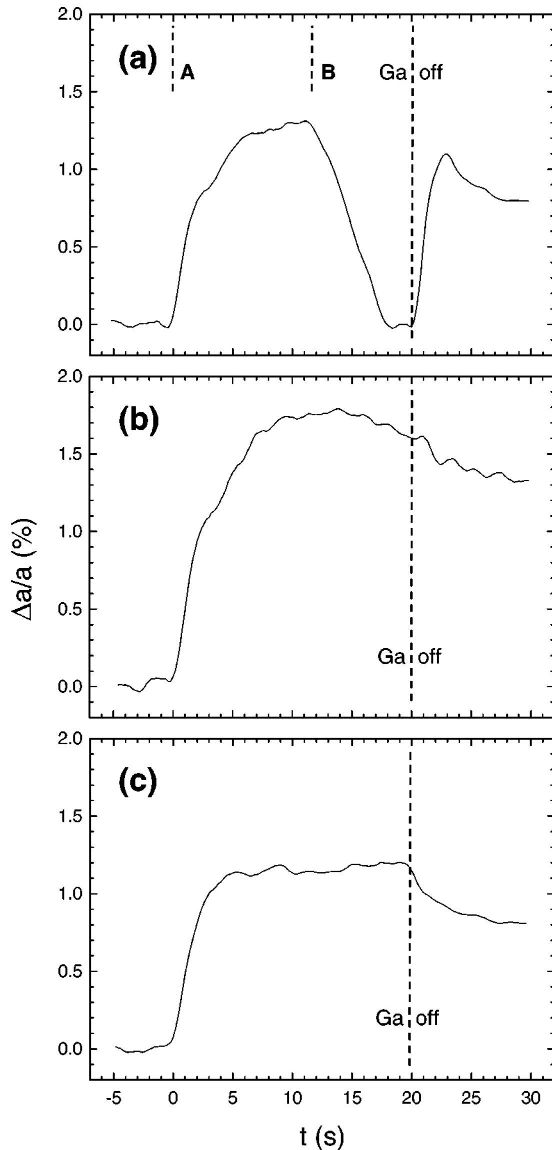


FIG. 9. Relative variation of the in-plane lattice parameter as a function of deposition time $t$ during the growth of a single layer of GaN on AlN substrate. (a) Ga-rich, (b) stoichiometry, (c) N-rich conditions. $T_S = 660\,°C$; the growth rate is 0.3 ML/s for (a) and (b) and 0.25 ML/s for (c), except after the metal flux is interrupted. Note the rapid relaxation occurring at the Ga interruption in (a).

plateau after the increase of stage (A). Near stoichoimetry, we find a somehow intermediate behavior: the decrease is weak, although visible [Fig. 9(b)]. Note that the RHEED pattern is affected under N-rich conditions: distinct Bragg spots appear, indicating growth front roughening. However, 2D growth is preserved under Ga-rich conditions, and the RHEED pattern remains streaky.

The amplitude of step (A) has been found to vary between 0.9% and 1.8% for different samples. No clear correlation between growth conditions and amplitude value has yet been deduced.

The effect of a subsequent growth interruption under an active N flux is presented in Fig. 9. An abrupt increase of $a$ by about 1% is observed for Ga-rich conditions [Fig. 9(a)], followed by a much smaller decrease that saturates very rapidly. In contrast, no significant change in $a$ is observed for N-rich conditions or near stoichiometry, apart from the weak saturating decrease [Figs. 9(b) and 9(c)].

These observations can be interpreted analogously to the case of AlN on GaN, described in the previous section: the reversibility of the relaxation in stages (A) and (B) demonstrates its elastic character through platelet formation [stage (A)]. Then, for Ga-rich growth, the platelets coalesce almost completely [stage (B)], and finally dislocations are introduced [stage (C)]. The characteristic length for irreversible relaxation is $\Lambda = 12$ nm, a value larger than that for AlN deposition (cf. Table I). On the other hand, no platelet coalescence takes place under N-rich conditions. In this situation, it is very difficult to separate elastic and plastic relaxation; therefore it is impossible to measure distinctly the irreversible part, as for Ga-rich growth.

For Ga-rich conditions, growth interruption under N flux leads again to platelet formation, consuming the accumulated excess Ga film on the surface. This explains the new increase of $a$ [Fig. 9(a)]. No such effect is observed when the Ga film is absent, i.e., for growth under N-rich conditions.

### B. Superlattice

Now consider a superlattice with alternate GaN and AlN layers of nominally equal thicknesses (3.2/3.2 nm) grown on the same AlN substrate (Fig. 10). Both GaN and AlN layers have been grown under metal-rich conditions. All steps (A), (B), and (C) are well visible during growth of the first GaN layer, as for a single layer. As a consequence of the above discussion, the reversible elastic steps (A) and (B) are now well distinguished from the irreversible introduction of dislocations (C), which appears as a continuous process throughout the entire superlattice. The dashed line displays the variation of the in-plane lattice parameter $a$ due to irreversible plastic relaxation. It converges at about 1.8%, slightly above the value of 1.3% expected for a superlattice with nominally equal layer thicknesses. It has to be noted that the metal excess has not been taken into account to compute the layer thickness, so the real thickness should deviate from these values. This may explain the difference in the expected and real asymptotic behavior.

During the interruption of the Ga deposition (nitrogen deposition alone) and as previously observed on a single layer, the in-plane lattice parameter deviates from the irreversible part, i.e., platelets are formed. We find again the transient ''overshooting'' of the relaxation just after the Ga shutter has been closed.

The growth of the AlN layers of the superlattice follows the same phenomenology as discussed in Sec. III. During AlN deposition, $a$ differs from the irreversible value due to elastic relaxation by platelet formation. When the Al flux is interrupted, $a$ evolves to the value corresponding to the irreversible part, since the layer has been grown under Al-rich conditions. Thus, the surface smoothens and the platelets disappear.

This process is periodic and reappears at each period of the superlattice: the only change is a gradual and irreversible

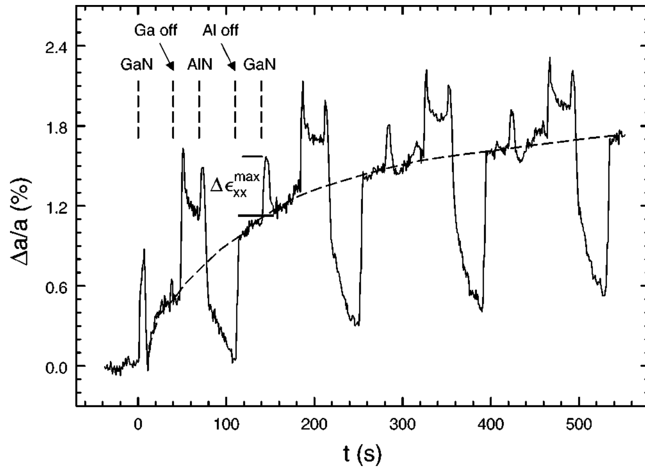


FIG. 10. Relative variation of the in-plane lattice parameter as a function of deposition time $t$ during the growth of a 3.2/3.2 nm AlN/GaN superlattice on an AlN substrate. Al- and Ga-rich conditions. $T_S = 640\,°C$; the growth rate is 0.3 ML/s, except after the metal flux is interrupted. A pronounced peak with the amplitude $\Delta\epsilon_{XX}^{max}$ appears when GaN starts to grow.

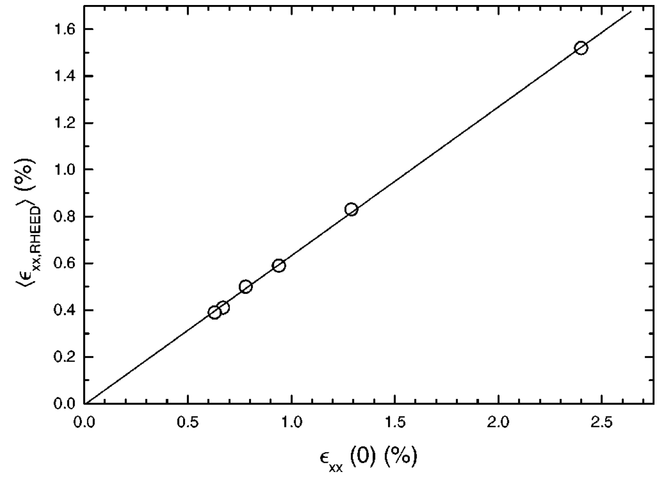


FIG. 11. Residual strain $\langle\epsilon_{xx,\mathrm{RHEED}}\rangle = \epsilon_{xx}(0) - \epsilon_{xx}^{max}$ on top of the platelets, as measured by RHEED, at the end of step (A) as a function of the residual misfit $\epsilon_{xx}(0)$ (as deduced from Fig. 10).

increase of the in-plane lattice parameter to its fully relaxed value of 1.8%. Albeit we have stated above that the maximum variation of the in-plane strain $\Delta\epsilon_{xx}^{max}$ due to elastic relaxation at the end of phase (A) of GaN growth may depend on the exact growth conditions of a specific sample, it is important to note that the residual strain on top of the platelets $\langle\epsilon_{xx,\mathrm{RHEED}}\rangle = \epsilon_{xx}(0) - \Delta\epsilon_{xx}^{max}$ depends linearly on the misfit $\epsilon_{xx}(0)$ experienced by the deposited GaN *for fixed growth conditions*. This linear dependence is illustrated in Fig. 11 for the data measured in Fig. 10. Interestingly, the extrapolation of the fit intersects the origin, as expected for elastic relaxation.

We can now summarize that during GaN growth platelets are immediately formed due to the misfit, then coalescence occurs only for Ga-rich growth conditions, and finally dislocations are formed. Platelets reappear after interruption of the Ga flux and during the consumption of the Ga excess.

Direct AFM imaging of the GaN layer surface (5 nm thick, Ga-rich growth) shows flat interconnected islands at a 12–14-nm scale (Fig. 12). Note that the corresponding RHEED pattern is streaky, consistent with the fact that the islands are flat. The height determined by AFM is in the range of 1.2–1.8 nm (5–7 ML). The density is of the order of $1\times10^{11}$ cm$^{-2}$, although it is difficult to obtain a precise value due to frequent island coalescence.

## V. DISCUSSION AND MODELING

There are three main mechanisms to relax biaxial strain in an epitaxial layer generated by a lattice-mismatched substrate:[49] (1) the introduction of interfacial dislocations, (2) the formation of a surface shape modulation, including, as a limit, islanding, and (3) the propagation of cracks (tensile stress) or film decohesion (compressive stress). Ceramics, as bulk AlN, usually deform through crack nucleation and propagation at temperatures below the brittle-to-ductile transition [mechanism (3)].[50] Several studies in different ceramics (but not precisely in AlN) have shown that the brittle-to-ductile transition occurs around a fraction 0.7–0.8 of the melting temperature $T_m$. Nevertheless, plastic deformation could occur at lower temperature, but the only way to avoid cracking at low and intermediate temperature ($<0.5T_m$) is to apply a large hydrostatic pressure ($\approx$1 MPa).[51]

Most of the experimental results on metals or semiconductors are compatible with mechanism (1) and involve dislocation movement: emission of sources from the surface, bowing of threading dislocations in the growth plane, emission from island edges at the triple junction between an island and the flat substrate. However, this process should be completely inhibited in group-III nitrides: in addition to the high-yield stress in ceramics, the hexagonal geometry of the system is such that the shear stress is zero on the usual glide planes. In AlN, for instance, the reported easy glide planes are the prismatic and basal planes,[51] in which the shear stress due to the biaxial strain is zero. Very occasional pyramidal glide has been observed at 500 °C (Ref. 51) but it seems too limited to explain the general phenomena of relaxation in group-III nitrides. Therefore, mechanism (1) can be excluded.

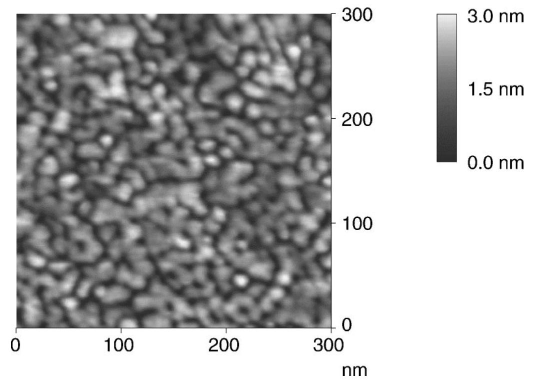


FIG. 12. AFM image of the top surface of a 4-nm-thick GaN layer grown on an AlN substrate. Ga-rich conditions, $T_S = 640\,°C$. Note that platelets are flat and start to coalesce.

Another way to relax misfit strain is to destabilize the growth front by producing surface modulation or eventually forming islands [mechanism (2)]. However, at first sight, 2D growth is maintained during both GaN and AlN deposition, since the RHEED pattern remain streaky and RHEED oscillations are observed. This seems to exclude the genuine formation of islands. Nonetheless, the formation of flat platelets, several monolayers in height, is fully consistent both with a rapidly appearing relaxation as well as with the observed streaky RHEED pattern. Reversibility is then explained by a ''filling process'' of the troughs between platelets. Based on this remark, we propose the following qualitative scheme from the previous observations.

During deposition, at a very early stage, platelets are formed. They are larger, more separated, and higher in the case of GaN than for AlN. Lateral sizes are in the range 10–20 nm with heights of several monolayers. In the case of AlN the top is flat and the edges sharp, possibly smoother for GaN.

These platelets may eventually coalesce during further growth after a typical deposition of 2–3 ML for GaN and 20 ML in case of AlN. Coalescence and surface smoothing depends critically of the stoichiometry of the deposited species and is fostered by a metal/nitrogen ratio $\Phi_{III}/\Phi_{N}>1$.

After stopping the metal deposition, the excess metal is used and forms new nitride material. As a consequence, the surface undergoes *smoothening* by filling up the troughs between platelets for AlN but *roughening* by formation of new GaN islands in case of GaN. This roughening is also evidenced by the more diffuse AlN on GaN interface, as measured by HRTEM.[42]

Dislocations are introduced with no well-defined critical thickness: the rate of introduction, as measured by $\Lambda$, is dependent of the stoichiometry ratio and, as a consequence, of the surface roughness. Irreversible relaxation is easier for N-rich growth, i.e., for rougher surfaces.

This qualitative scheme is summarized on the schematic views in Figs. 13 and 14. It should be emphasized that these platelets are to be distinguished from the truncated pyramidal islands observed at higher temperature.[36] The height of the platelets considered here is smaller, their density much higher, and the coverage close to 1. They do appear right at the beginning of the deposition and, as they are flat, the growth remains in a pseudo-2D mode, with nuclei formation on top of the platelets. Also, the RHEED pattern maintains its overall streaky character.

Two points require more attention and shall be discussed in the following: (1) can we deduce more quantitative information from the elastic (reversible) relaxation observed on the in-plane lattice parameter measurement and (2) how are new dislocations (irreversible relaxation) introduced in nitrides?

### A. Elastic relaxation through platelets

Several calculations of the strain distribution inside isolated or interacting islands deposited on a substrate with a given misfit $f_0$ were made.[47,52–54] Yet, the only tractable analytical form that takes into account the deformation of the substrate is the one given by Kern and Müller.[46] Although it is limited to one-dimensional elongated ribbons, it will give a good order of magnitude estimation of the relaxation of the top layers. These authors show that the strain in the $x$ direction (cf. Fig. 15) $\epsilon_{xx}^{f}$ in an infinitely long ribbon of height $h_R$ and width $l_R$, deposited coherently on a substrate having a misfit $f_0$, is given by

$$\epsilon_{xx}^{f}(x,N)=\epsilon_{xx}^{f}(x,0)\langle M_1\rangle^{N}, \quad (1)$$

with

$$\langle M_1\rangle = 1-\frac{2\pi\tau}{N_T}+\left(1+\sqrt{\frac{2\pi\tau}{N_T}}\right)^2 \exp\left(-\sqrt{\frac{2N_T}{\pi\tau}}\right), \quad (2)$$

where $\tau=h_R/l_R$ is the aspect ratio; $N$ defines the number of monolayers from the surface and varies from $N=0$ to $N=N_T\equiv h_R/a$, the total number of monolayers included in the ribbon of height $h_R$. As in Ref. 46, the ratio of the Young moduli and the Poisson ratios have been approximated to 1

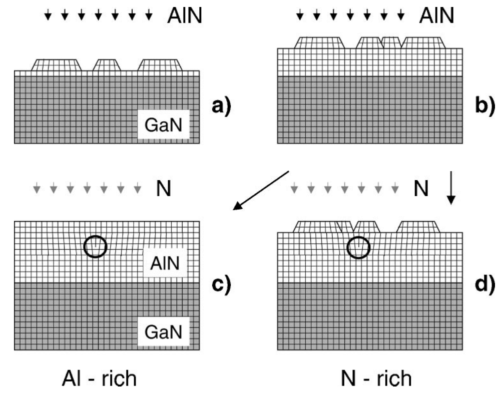


FIG. 13. Schematic representation of the growth of AlN on GaN. (a) Early formation of flat AlN platelets in tension with elastic inward relaxation at the edges and (b) further growth with partial coalescence of the platelets. (c) Dislocation introduction (irreversible relaxation) and smoothing of the surface under nitrogen deposition after Al-rich growth, while (d) dislocation introduction with no smoothing under nitrogen deposition after N-rich growth.

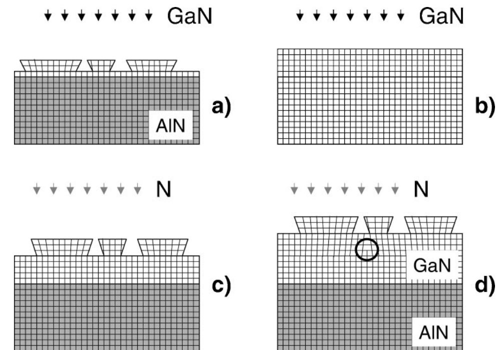


FIG. 14. Schematic representation of the growth of GaN on AlN. (a) Early formation of flat GaN platelets in compression and outward elastic relaxation and (b) smoothing during further deposition. (c) Platelets reappear after $N$ only deposition. (d) For larger thicknesses, dislocations are introduced and irreversible relaxation is observed.

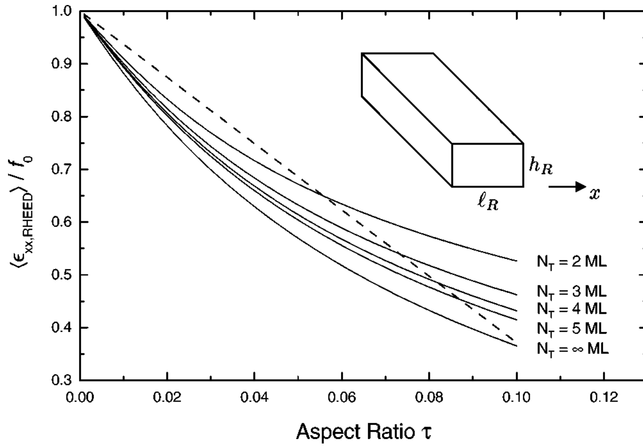


FIG. 15. Calculated apparent in-plane lattice parameter relaxation due to platelets, $N_T$ ML high, with aspect ratio $\tau$. $f_0$ is the initial misfit between the material of the platelet and the substrate on which the platelet is sitting. The solid lines are calculated following Eq. (6) and the dashed line shows the linear approximation given in Eq. (7).

(depending on the reference, AlN has elastic constants 10% to 20% larger than GaN; see, for instance, Refs. 55 and 56).

The strain at the interface $\epsilon_{xx}^f(x,0)$ is equal to $f_0$ when the substrate is considered rigid and otherwise the average (over $x$) strain at the interface is given by

$$\langle \epsilon_{xx}^f \rangle = f_0 \langle M \rangle, \tag{3}$$

with

$$\langle M \rangle = 1 - \frac{2}{P^2} + \left(1 + \frac{\sqrt{2}}{P}\right)^2 \exp(-P\sqrt{2}), \tag{4}$$

and, neglecting the surface tension,

$$P^2 = \frac{N_T \ln\langle M_1 \rangle}{\pi\tau[\langle M_1 \rangle^{N_T} - 1]}, \tag{5}$$

where $N_T$ is the number of total monolayer considered in the ribbon.

The strain measured by RHEED is an average over $x$ and, at maximum, over the last 3 ML (this will be $\approx 1$ nm, a typical penetration depth of the electrons at grazing incidence) and will be given by

$$\langle \epsilon_{xx,\mathrm{RHEED}}^f \rangle = \langle \epsilon_{xx}^f \rangle \tfrac{1}{3} \sum_{i=0}^{2} \langle M_1 \rangle^{N_T - i}. \tag{6}$$

As remarked by Kern and Müller, the average strain in the substrate is close to zero, so that the RHEED pattern is only sensitive to the strain inside the ribbon. From Eq. (6), the averaged strain measured by the RHEED is plotted as a function of the aspect ratio $\tau$ and the height (or total number of monolayers) in Fig. 15.

A simple first-order approximation can be obtained by considering only the topmost layer, supposing a rigid substrate, and developing formulas (1) and (2) for $\tau/N_T \ll 1$, i.e., for ribbons that are wide compared to atomic distances:

$$\langle \epsilon_{xx}^f \rangle = f_0(1 - 2\pi\tau). \tag{7}$$

This linear approximation is shown in Fig. 15 as a dashed line.

The apparent strain, even for a completely coherent ribbon, differs from the misfit $f_0$. The difference varies approximately linearly with the aspect ratio $\tau$, at least for small values, i.e., for ribbons that are sufficiently flat. In this limit, the strain depends on $\tau$ and the misfit $f_0$ only. The difference between the slope and that of the linear approximation in Eq. (7) is due to the fact that we have assumed the substrate rigid in the latter case. However, for aspect ratios larger than 0.02, the strain becomes explicitly dependent on the absolute value of the island height, particularly for $N_T$ smaller than 5 ML.

Is this calculation directly comparable to RHEED measurements? First, one should be aware that one lateral dimension is missing. However, the order of magnitude should be correct when corner effects are small compared to the platelet size, i.e., for small enough aspect ratio, as considered here. Furthermore, the surface probed by RHEED should not include the substrate or epitaxial material at different heights, a condition that is fulfilled for layer-by-layer growth. The HRTEM cross section in Fig. 7 indicates a rather flat growth front even when the layer is not continuous. The edges of the platelets are sharp and their density is high, so it seems safe to assume that the regions between platelets are shadowed by the platelets and do not contribute to the RHEED pattern. In the case of GaN, AFM imaging (Fig. 12) shows that platelets are also flat and the ribbon model should be appropriate. This is also corroborated by the absence of evidence for facets in the RHEED pattern, as opposed to truncated pyramidal-shaped GaN islands grown at higher temperatures in a Stranski-Krastanow mode.[36]

Based on these approximations, we can use the experimental results in two situations: For the deposition of AlN on GaN substrate in N-rich conditions, the typical absolute value of the platelets' height ($h = 0.8$ nm) and diameter ($l = 20$ nm) can be extracted from the AFM micrograph in Fig. 6(a). This leads to $N_T = 3$ ML and $\tau = 0.04$. Using Eq. (6) (cf. Fig. 15), we then deduce a value of the residual strain of $\langle \epsilon_{xx,\mathrm{RHEED}}^f \rangle / f_0 = 0.68$, corresponding to an elastic relaxation that should be observed by RHEED of about $\Delta a/a = (1 - 0.68) \times 2.4\% = 0.8\%$. Since the layer depicted in Fig. 6(a) has been grown under conditions similar to those of the layer in Fig. 2(c) (the layer thickness of 4 nm corresponds to a deposition time of 50 s), we conclude that the observed relaxation of about 1.7% must contain both elastic and plastic contributions.

It is noticeable that the calculated elastic relaxation of the platelets grown in N-rich conditions [Fig. 6(a)] is almost equal to the elastic relaxation right after stage (A) observed in near-stoichiometric and in Al-rich conditions [see Figs. 2(a) and 2(b)]. We can therefore assume that the platelet morphology of the AlN surface shown in Fig. 6(a) may also be representative of the transient platelet morphology during growth in near-stoichiometric conditions. Using Eq. (6) (cf. Fig. 15), it can be deduced that the aspect ratio of the platelets grown in Al-rich or near-stoichiometric conditions—which relax by about 0.8%—must vary in the range between

0.035 and 0.051, depending on the platelets' height. However, as far as their absolute height and diameter are concerned, it cannot be discarded that they moderately depend on the Al/N ratio.

For the deposition of GaN on AlN substrate, the maximum elastic relaxation is typically of the order of $\Delta a/a = 1.2\%$, thus we obtain $\langle \epsilon^{f}_{xx,\mathrm{RHEED}} \rangle / f_0 = 1 - 1.2\%/2.4\% = 0.5$. This is consistent with an aspect ratio varying from 0.063 to 0.11, when assuming a platelet height between $N_T = \infty$ and $N_T = 2$ ML, respectively. Then, taking into account the typical platelet diameter measured by AFM ($l = 13$ nm), one can check if the assumed platelet height between 2 and $\infty$ ML is in agreement with the observed relaxation. We find that only a value of 4–5 ML passes this self-consistency check and is consistent with the curves in Fig. 15. This value is only slightly smaller than that given by AFM (5–7 ML), which can be explained by the observed coalescence of some platelets, reducing the edge elastic relaxation.

For GaN deposition, Fig. 11 shows that the residual strain on top of the platelets is strictly proportional to the misfit: as a consequence the geometry of the platelets has to remain constant and is not varying with the misfit strain [see Eq. (3)]. One can infer that kinetic parameters governing platelet growth and shape play an important role and prevail over elastic effects. This elucidates also the slight variation of the relaxation amplitude between different samples, since exact kinetic parameters may slightly vary, as it is difficult to reproduce, i.e., $\Phi_{\mathrm{III}}/\Phi_{\mathrm{N}}$ with high precision. Also, the substrate step density may influence platelet growth, a parameter that is at present still ill-controlled for the growth of group-III nitrides. As stated in Sec. III B, no such correlation between elastic and inelastic relaxation has been observed for AlN grown on GaN. Then, this discussion seems to be less applicable to the case of AlN deposition, for which the platelet morphology appears strain dependent.

### B. Dislocation-introduction mechanism

Several attempts to measure a critical thickness in growing nitride heterostructures are reported in the literature.[27,30,32,34] Its value varies from 1 to 9 nm. The above discussion shows clearly that it is difficult, if not impossible, to define a unique critical thickness in the usual sense, because of the early apparition of flat platelets. Moreover, the sensitivity of the growth process (even for the same growth method) to the exact metal/N ratio could also explain the different values reported. The above results, demonstrating the mixture of elastic and plastic relaxation during the early stages of deposition, prevent us from trying to define a general value for the thickness at which plastic relaxation begins. For AlN growth, the transition between steps (B) and (C) depends on the metal/N ratio, as illustrated in Fig. 2. Near stoichiometry, a slope change is observed after a deposition time of 80 s, which corresponds to a thickness of 6 nm: this will give an upper limit for the critical thickness. A lower limit could be defined at the end of step (A), at around 3–4 ML. In between these two values, platelets may evolve and eventually coalescence may already occur as well as dislocations may already be formed: the measurement of the in-plane lattice parameter is not sufficient to discriminate between both phenomena.

The irreversible part of the evolution of $a$ during stage (C) is close to a pure exponential evolution in any situation considered. The variation of the strain $\epsilon$ as a function of the layer thickness $h$ is then given by an equation of the type

$$\epsilon(h) = \epsilon_0 \exp\left( - \frac{h - h_c}{\Lambda} \right), \quad (8)$$

where $\epsilon_0$ is the total amplitude of the relaxation, $h_c$ is an apparent critical thickness, and $\Lambda$ is the characteristic thickness for irreversible relaxation. Experimental values of the phenomenological parameters $\epsilon_0$ and $\Lambda$ are given in Table I. These parameters have a direct physical meaning and can be related to the local dislocation density $\rho(h)$ as follows:

$$\rho(h) = \frac{\epsilon_0}{b_\perp \Lambda} \exp\left( - \frac{h - h_c}{\Lambda} \right), \quad (9)$$

where $b_\perp$ is the Burgers vector component parallel to the interface and perpendicular to the dislocation line. Pure edge dislocations along the three equivalent $\langle 10\bar{1}0 \rangle$ directions with perpendicular Burgers vectors $\mathbf{b} = \frac{1}{3}\langle \bar{1}2\bar{1}0 \rangle$ are able to relax biaxial strain. Indeed, these dislocations were observed in multilayers by HRTEM (Fig. 1). From Eq. (9), we can deduce that the first layers ($h$ close to $h_c$) of GaN grown on AlN substrates would have given a dislocation density of $7 \times 10^{11}\,\mathrm{cm}^{-2}$, using the measured values for GaN deposition and $b_\perp = a_{\mathrm{GaN}} = 0.31$ nm. It is worth noting that this maximum density corresponds to an average distance between dislocations of 12 nm, a value comparable to the typical platelet diameter determined by AFM.

A phenomenological model, explaining the exponential decrease has been proposed by Feuillet *et al.*:[33] the probability of creating a dislocation is proportional to the local misfit experienced by the deposited material. It is easy to show that a pure exponential relaxation should then be observed. However, the creation mechanism has not been explained. If we exclude the usual mechanism of nucleation and glide for the reasons discussed above, two alternatives can be proposed.

First, as-grown threading dislocations from the substrate could be bent from the growth direction to the interface plane. Indeed, MOCVD pseudosubstrates do contain the appropriate edge dislocations with the correct Burgers vector $\mathbf{b} = \frac{1}{3}\langle \bar{1}2\bar{1}0 \rangle$. Nevertheless, their typical density is of the order of $10^9\,\mathrm{cm}^{-2}$, a value much lower than that required to account for the observed relaxation.

Second, dislocations may be nucleated at the junction of two growing platelets. As illustrated in Fig. 16, when two strained platelets are close together, the distance between the edge atoms of each platelet is modified compared to that between inner atoms due to edge relaxation. For platelets in tension (compression), this distance is larger (smaller). Thus, it is favorable for adatoms to nucleate an edge dislocation with a positive (negative) Burgers vector at the trough between two islands.

The inward (outward) relaxation is proportional to the local misfit $\epsilon(h)$. Therefore, the probability of generating a

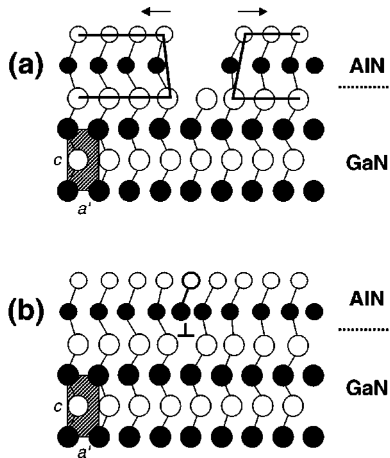


FIG. 16. Schematic model of the nucleation of a misfit dislocation between two platelets in tension (AlN on GaN): (a) before coalescence, (b) after coalescence. Note that inward relaxation opens up the gap between the two platelets and favors adatom nucleation at this site, promoting dislocation nucleation.

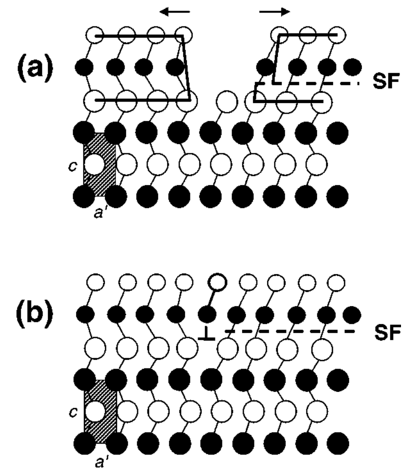


FIG. 17. Schematic model of the nucleation of a misfit dislocation between an hexagonal platelet and a locally cubic one, i.e., having a stacking fault (SF), under tension: (a) before coalescence, (b) after coalescence. For favorable stacking fault vectors, the opening of the gap between the two platelets is even larger than that for Fig. 16 and dislocation nucleation is easier.

new dislocation in order to relax the strain should be a function of $\epsilon(h)$. To prove that this function is approximately linear, as observed experimentally, is beyond the scope of the present study and would require atomic calculations. However, this dislocation nucleation mechanism is plausible since it requires no dislocation glide. Furthermore, it gives the right order of magnitude for the dislocation density in the initial stage of high misfit ($\approx$2%) for the measured platelet diameter.

The interdependency of platelet formation and dislocation production during growth is well illustrated by the influence of metal/N ratio on $\Lambda$ and, as a consequence, on $\rho(h)$ (see Table I). It has been shown that N-rich conditions enhance the formation of stacking faults.[40,57] The coexistence of hexagonal and cubic islands has also been experimentally observed by scanning tunneling microscopy for the 2D nucleation growth mode of GaN.[58] In this case, the distance between two adjacent platelets (one in hexagonal position and one in cubic position) could be larger (smaller) than for two hexagonal platelets and would further increase the probability to nucleate the appropriate positive (negative) dislocation (see Fig. 17).

We remark that a related mechanism of dislocation nucleation has been evoked for the plastic relaxation of compressively strained islands grown in Stranski-Krastanow mode in the Ge/Si (Ref. 59) and InAs/GaAs (Ref. 60) systems. It has been found that dislocations are most likely formed at the corners of the islands, where the strain is most concentrated. This has been confirmed by theoretical modeling.[61,62]

## VI. CONCLUSION

The relaxation of (0001)/GaN/AlN heterostructures has been studied by *in situ* reflection high-energy electron diffraction measurements and *ex situ* atomic-force and transmission electron microscopy. It has been found that the PAMBE growth mechanism in III-V nitrides is more complex than that in other III-V materials. Although for GaN on AlN and AlN on GaN pseudo-2D growth is commonly observed and controlled, the variation of the in-plane lattice parameter during the initial stages of epilayer growth can be only accounted for by considering both elastic and plastic relaxation processes. The elastic part of the relaxation is explained by the dynamic formation of platelets.

As far as plastic relaxation is concerned, the combination of large strain, high Schwoebel barrier, and low dislocation mobility leads to a different relaxation mechanism: the tendency to form platelets as a dynamic process during growth is fostering the formation of misfit dislocations. This new understanding could help to grow the desired structures: high platelet density and/or stacking faults, i.e., growth under N-rich conditions, would concentrate dislocation formation in a specific location. Low density of platelets with small aspect ratio would hamper dislocation formation and introduce a larger critical thickness. Growth under near-stoichiometric conditions would favor this latter case. It is reasonable to suggest that deposition rate is another parameter to control platelets. A higher deposition rate would generate higher platelet density and smaller platelet size. Finally, the important role of an interruption of metal deposition during heterostructure growth is now understood: after AlN deposition, it helps to suppress the platelets formed dynamically and further GaN growth could start on a smooth surface. However, after GaN growth, the excess Ga is consumed and new platelets are formed. As a consequence, further AlN growth is producing a less sharp interface compared to the GaN on AlN interface. On the other hand, the absence of any metal interruption after GaN growth may induce $Al_xGa_{1-x}N$ alloy formation due to the excess Ga and is not recommended.

## ACKNOWLEDGMENTS

We would like to acknowledge M. Arlery for the electron microscopy observations and for giving us unpublished results (Figs. 1 and 7). We also thank Y. Samson for use of the AFM facility.

*Corresponding author. Electronic address: bdaudin@cea.fr

[1] S. Nakamura and G. Fasol, *The Blue Laser Diode* (Springer, Berlin, 1999).
[2] A. Kinoshita, H. Hirayama, M. Ainoya, Y. Aoyagi, and A. Hirata, Appl. Phys. Lett. **77**, 175 (2000).
[3] Y.-K. Song, M. Diagne, H. Zhou, A. V. Nurmikko, R. P. Schneider, and T. Takeuchi, Appl. Phys. Lett. **77**, 1744 (2000).
[4] T. Someya, R. Werner, A. Forchel, M. Catalano, R. Cingolani, and Y. Arakawa, Science **285**, 1905 (1999).
[5] Y.-K. Song, H. Zhou, M. Diagne, A. V. Nurmikko, R. P. Schneider, C. P. Kuo, M. R. Krames, R. S. Kern, C. Carter-Coman, and F. A. Kish, Appl. Phys. Lett. **76**, 1662 (2000).
[6] E. Monroy, M. Hamilton, D. Walker, P. Kung, F. J. Sánchez, and M. Razeghi, Appl. Phys. Lett. **74**, 1171 (1999).
[7] J. L. Pau, E. Monroy, F. B. Naranjo, E. Muñoz, F. Calle, M. A. Sánchez-García, and E. Calleja, Appl. Phys. Lett. **76**, 2785 (2000).
[8] E. J. Tarsa, P. Kozodoy, J. Ibbetson, B. P. Keller, G. Parish, and U. K. Mishra, Appl. Phys. Lett. **77**, 316 (2000).
[9] Y. F. Wu, B. P. Keller, P. Fini, S. Keller, T. J. Jenkins, L. T. Kehias, S. P. DenBaars, and U. K. Mishra, IEEE Electron Device Lett. **19**, 50 (1998).
[10] M. J. Murphy, K. Chu, H. Wu, W. Yeo, W. J. Schaff, O. Ambacher, L. F. Eastman, T. J. Eustis, J. Silcox, R. Dimitrov, and M. Stutzmann, Appl. Phys. Lett. **75**, 3653 (1999).
[11] J. B. Limb, H. Xing, B. Moran, L. McCarthy, S. P. DenBaars, and U. K. Mishra, Appl. Phys. Lett. **76**, 2457 (2000).
[12] C. Kisielowski, in *Gallium Nitride (GaN) II*, edited by J. I. Pankove and T. D. Moustakas, Vol. 57 of Semiconductors and Semimetals (Academic, San Diego, 1999), p. 275.
[13] F. Bertram, T. Riemann, J. Christen, A. Kaschner, A. Hoffmann, C. Thomsen, K. Hiramatsu, T. Shibata, and N. Sawaki, Appl. Phys. Lett. **74**, 359 (1999).
[14] Jin Seo Im, H. Kollmer, J. Off, A. Sohmer, F. Scholz, and A. Hangleiter, Phys. Rev. B **57**, R9435 (1998).
[15] M. Leroux, N. Grandjean, J. Massies, B. Gil, P. Lefebvre, and P. Bigenwald, Phys. Rev. B **60**, 1496 (1999).
[16] J. Simon, R. Langer, A. Barski, and N. T. Pelekanos, Phys. Rev. B **61**, 7211 (2000).
[17] F. Widmann, J. Simon, B. Daudin, G. Feuillet, J. L. Rouvière, N. T. Pelekanos, and G. Fishman, Phys. Rev. B **58**, R15 989 (1998).
[18] B. Damilano, N. Grandjean, F. Semond, J. Massies, and M. Leroux, Appl. Phys. Lett. **75**, 962 (1999).
[19] H. Amano, K. Hiramatsu, and I. Akasaki, Jpn. J. Appl. Phys., Part 2 **27**, L1384 (1988); T. Detchprohm, K. Hiramatsu, K. Itoh, and I. Akasaki, *ibid.* **31**, L1454 (1992); K. Hiramatsu, T. Detchprohm, and I. Akasaki, Jpn. J. Appl. Phys., Part 1 **32**, 1528 (1993).
[20] C. Kim, I. K. Robinson, J. Myoung, K.-H. Shim, M.-C. Yoo, and K. Kim, Appl. Phys. Lett. **69**, 2358 (1996).
[21] O. Gfrorer, T. Schlusener, V. Harle, F. Scholz, and A. Hangleiter, Mater. Sci. Eng., B **43**, 250 (1997).
[22] X. H. Wu, P. Fini, E. J. Tarsa, B. Heying, S. Keller, U. K. Mishra, S. P. DenBaars, and J. S. Speck, J. Cryst. Growth **190**, 231 (1998).
[23] R. L. Headrick, S. Kycia, A. R. Woll, J. D. Brock, and M. V. Ramana Murty, Phys. Rev. B **58**, 4818 (1998).
[24] I. H. Lee, I. H. Choi, C. R. Lee, E. J. Shin, D. Kim, S. K. Noh, S. J. Son, K. Y. Lim, and H. J. Lee, J. Appl. Phys. **83**, 5787 (1998).
[25] S. Hearne, E. Chason, J. Han, J. A. Floro, J. Figiel, J. Hunter, H. Amano, and I. S. T. Tsong, Appl. Phys. Lett. **74**, 356 (1999).
[26] A. V. Dobrynin, J. Appl. Phys. **85**, 1876 (1999).
[27] C. Kim, I. K. Robinson, J. Myoung, K.-H. Shim, and K. Kim, J. Appl. Phys. **85**, 4040 (1999).
[28] A. R. Woll, R. L. Headrick, S. Kycia, and J. D. Brock, Phys. Rev. Lett. **83**, 4349 (1999).
[29] D. C. Reynolds, D. C. Look, B. Jogai, J. E. Hoelscher, R. E. Sherriff, and R. J. Molnar, J. Appl. Phys. **88**, 1460 (2000).
[30] Z. Sitar, M. J. Paisley, B. Yan, J. Ruan, W. J. Choyke, and R. F. Davis, J. Vac. Sci. Technol. B **8**, 316 (1990).
[31] A. D. Bykhovski, B. L. Gelmont, and M. S. Shur, J. Appl. Phys. **78**, 3691 (1995).
[32] N. Grandjean and J. Massies, Appl. Phys. Lett. **71**, 1816 (1997).
[33] G. Feuillet, B. Daudin, F. Widmann, J. L. Rouvière, and M. Arlery, J. Cryst. Growth **190**, 142 (1998).
[34] R. Langer, A. Barski, A. Barbier, G. Renaud, M. Leszczynski, I. Grzegory, and S. Porowski, J. Cryst. Growth **205**, 31 (1999).
[35] R. Langer, A. Barski, J. Simon, N. T. Pelekanos, O. Konovalov, R. André, and Le Si Dang, Appl. Phys. Lett. **74**, 3610 (1999).
[36] B. Daudin, F. Widmann, G. Feuillet, Y. Samson, M. Arlery, and J. L. Rouvière, Phys. Rev. B **56**, R7069 (1997).
[37] J. W. Matthews and A. E. Blakeslee, J. Cryst. Growth **27**, 118 (1974); **29**, 273 (1975); **32**, 265 (1976).
[38] R. People and J. C. Bean, Appl. Phys. Lett. **47**, 322 (1985).
[39] T. Zywietz, J. Neugebauer, and M. Scheffler, Appl. Phys. Lett. **73**, 487 (1998).
[40] E. J. Tarsa, B. Heying, X. H. Wu, P. Fini, S. P. DenBaars, and J. S. Speck, J. Appl. Phys. **82**, 5472 (1997).
[41] B. Heying, R. Averbeck, L. F. Chen, E. Haus, H. Riechert, and J. S. Speck, J. Appl. Phys. **88**, 1855 (2000).
[42] M. Arlery, Ph.D. thesis, Université Joseph Fourier Grenoble I, 1998.
[43] P. W. Deelman, T. Thundat, and L. J. Schowalter, Appl. Surf. Sci. **104/105**, 510 (1996).
[44] S. Guha, A. Madhukar, and K. C. Rajkhumar, Appl. Phys. Lett. **57**, 2110 (1990).
[45] C. W. Snyder, B. G. Orr, D. Kessler, and L. M. Sander, Phys. Rev. Lett. **66**, 3032 (1991).
[46] R. Kern and P. Müller, Surf. Sci. **392**, 103 (1997).
[47] J. Massies and N. Grandjean, Phys. Rev. Lett. **71**, 1411 (1993).
[48] J. Eymery, S. Tatarenko, N. Bouchet, and K. Saminadayar, Appl. Phys. Lett. **64**, 3631 (1994).
[49] H. P. Strunk, M. Albrecht, S. Christiansen, W. Dorsch, U. Hormann, B. Jahnen, and T. Remmele, Phys. Status Solidi A **171**, 215 (1999).
[50] S. J. Hearne, J. Han, S. R. Lee, J. A. Floro, D. M. Follstaedt, E. Chason, and I. S. T. Tsong, Appl. Phys. Lett. **76**, 1534 (2000).
[51] V. Audurier, J. L. Demenet, and J. Rabier, Philos. Mag. A **77**, 825 (1998).
[52] M. Grundmann, O. Stier, and D. Bimberg, Phys. Rev. B **52**, 11 969 (1995).
[53] T. Saito, J. N. Schulman, and Y. Arakawa, Phys. Rev. B **57**, 13 016 (1998).
[54] A. Ponchet, D. Lacombe, L. Durand, D. Alquier, and J. M. Cardonna, Appl. Phys. Lett. **72**, 2984 (1998).
[55] K. Kim, W. R. L. Lambrecht, and B. Segall, Phys. Rev. B **53**, 16 310 (1996).

[56] C. Deger, E. Born, H. Angerer, O. Ambacher, M. Stutzmann, J. Hornsteiner, E. Riha, and G. Fischerauer, Appl. Phys. Lett. **72**, 2400 (1998).
[57] F. Widmann, B. Daudin, G. Feuillet, N. Pelekanos, and J. L. Rouvière, Appl. Phys. Lett. **73**, 2642 (1998).
[58] M. H. Xie, S. M. Seutter, W. K. Zhu, L. X. Zheng, H. Wu, and S. Y. Tong, Phys. Rev. Lett. **82**, 2749 (1999).
[59] F. K. LeGoues, M. C. Reuter, J. Tersoff, M. Hammar, and R. M. Tromp, Phys. Rev. Lett. **73**, 300 (1994); Appl. Phys. Lett. **67**, 2317 (1995).
[60] Y. Chen, X. W. Lin, Z. Lilienthal-Weber, J. Washburn, J. F. Klemm, and J. Y. Tsao, Appl. Phys. Lett. **68**, 111 (1996).
[61] H. T. Johnson and L. B. Freud, J. Appl. Phys. **81**, 6081 (1997).
[62] B. J. Spencer and J. Tersoff, Appl. Phys. Lett. **77**, 2533 (2000).